

# The stability of evaporating thin liquid films in the presence of surfactant.

## I. Lubrication approximation and linear analysis

Krassimir D. Danov<sup>a)</sup>

Laboratory of Thermodynamics and Physicochemical Hydrodynamics, Faculty of Chemistry, Sofia University, 1 J. Bourchier Ave., 1126 Sofia, Bulgaria

Norbert Alleborn, Hans Raszillier, and Franz Durst

Lehrstuhl für Strömungsmechanik, Universität Erlangen-Nürnberg, Cauerstraße 4, D-91058 Erlangen, Germany

(Received 31 October 1996; accepted 26 August 1997)

The dynamics of an evaporating wetting liquid film in the presence of dissolved surfactant is investigated. The solid substrate is planar and is subjected to heating. The liquid–vapor interface is a two-dimensional continuum characterized by specific adsorption, interfacial viscosity, and surface tension, which depend on the surfactant subsurface concentration and temperature. In the case of small density, viscosity, and thermal conductivity of the vapor phase (compared to the respective values for the liquid phase), at small Reynolds and large Peclet numbers and for thin films, the lubrication approximation model can be applied. The effect of the van der Waals disjoining pressure is taken into account. The appearing dimensionless groups, defined in terms of the real physical parameters, can vary by several orders of magnitude depending on the film initial thickness, temperature difference, and type of surfactants. The developed linear theory describes the competition among the various instabilities. The numerical solution of the evolution equation provides information about the critical film thickness, critical lateral wave number, and time for rupture. The influence of the interfacial mass loss due to evaporation, the van der Waals attraction, the Marangoni effects due to thermal and concentration gradients, and the interfacial viscous friction upon the critical film thickness is discussed. © 1998 American Institute of Physics.

[S1070-6631(97)03212-1]

## I. INTRODUCTION

The stability of thin liquid films (of thickness in the range between 10 nm and 20  $\mu\text{m}$ ) is an important problem in diverse areas of science and technology. Technological and biological examples include foam and emulsion stability;<sup>1</sup> displacement of crude oil by gas and foam from rock pores;<sup>2</sup> safety of light-water cooled nuclear power plants;<sup>3</sup> adsorption refrigeration, where some surface active agents increase the capacity of adsorption cooling machines;<sup>4</sup> coating<sup>5</sup> and deposition processes in certain high technologies, semiconductor chip deposition,<sup>6</sup> and fiber optic coating;<sup>7</sup> and the rupture of the tear film in the human eye.<sup>8</sup> As a result of thermal fluctuations or outer mechanical disturbances the surface of the film is deformed. When the local film thickness is small, the surface forces<sup>9</sup> can amplify the interfacial corrugations.<sup>10</sup> Evaporation from or condensation on the interface of a wetting liquid film has an additional destabilizing effect.<sup>11</sup> The mass transfer into or onto the film phase can influence significantly the magnitude of the interfacial corrugations.<sup>12</sup>

A surfactant monolayer spread at a fluid interface damps the surface wave motion. This phenomenon is due to the fact that as the monolayer is compressed and expanded, the local variations of the adsorption lead to local variations of the interfacial tension. The combination of the resulting surface

tension gradients (Marangoni effects) with the effect of the interfacial viscosity results in damping of the surface waves.

The inability to obtain an analytical solution of the problem for the hydrodynamic instability of thin liquid films makes the linear analysis one of the most widely applied mathematical procedures.<sup>13,14</sup> Due to the different lateral dimensions, the instability of the wetting film on a substrate and that of the thin liquid film between two deformed droplets are influenced by different forces. The wavelengths in films between two deformed emulsion droplets or small bubbles are bounded by the film radius and the gravity force does not influence the stability. In the case of falling films and films on a solid substrate the waves have unbounded lateral dimensions and the thermal and gravity instabilities are much more pronounced. The full linear analysis of the fluctuations of the thickness of stationary quasiequilibrium plane-parallel thin liquid film between two different phases is given by Maldarelli *et al.*<sup>10</sup> Those authors derived a dispersion relation that includes the influence of the van der Waals and electrostatic interactions and the Marangoni effect due to the surfactant redistribution. De Vries<sup>15</sup> was the first who pointed out that the local fluctuations of the film thickness lead to two opposite effects: a positive contribution to the free energy due to the increase of the film area and negative contribution resulting from the increased negative surface energy of interaction in the thinner part of the corrugated film. Vrij<sup>16</sup> and Vrij and Overbeek<sup>17</sup> defined the transitional thickness of the film, which corresponds to the zero rate of growth of the corrugation. After that, finite time is needed for the two surfaces to touch each other; during

<sup>a)</sup>To whom correspondence should be addressed. Krassimir D. Danov, Laboratory of Thermodynamics and Physicochemical Hydrodynamics, Faculty of Chemistry, Sofia University, 1 J. Bourchier Ave., 1126 Sofia, Bulgaria. Telephone: (359)-2-962-53-10; Fax: (359)-2-962-56-43; Electronic mail: KRASSIMIR.DANOV@LTPH.BOL.BG

this period of time the average thickness of the film will continue to decrease. The theoretical development of this idea was made by Ivanov *et al.*,<sup>18,19</sup> who investigated the stability of a thin foam plane-parallel film in the whole process of its drainage. One way to generalize this work is to employ the nonlinear analysis of stability, similarly to the treatment of Yantsios and Higgins<sup>20</sup> for wetting film. The destabilizing effect of the diffusion transfer of solutes (alcohol, acetic acid, and acetone) from one bulk phase to the other, across the interface, was studied experimentally.<sup>21,22</sup> The observed destabilization of the films can be attributed to the appearance of Marangoni instability.<sup>12</sup> Lin and Brenner<sup>8</sup> examined the role of the heat and mass transfer in an attempt to check the hypothesis of Holly<sup>23</sup> that the Marangoni instability can cause the rupture of tear films. Their analysis was extended by Castillo and Velarde,<sup>24</sup> who showed that the heat and mass transfer drastically reduce the threshold for the appearance of Marangoni convection.

The linear stability analysis of a wetting film in the absence of surfactants was performed by Jain and Ruckenstein<sup>25</sup> and was generalized for surfactant stabilized films in Ref. 26. It was found that the dynamic interfacial characteristics (surface diffusivity and viscosity, Gibbs elasticity, and instantaneous adsorption) are more important factors than the value of the surface tension itself. Gumerman and Homsy<sup>27</sup> have extended this analysis by including substrate and drainage effects. Williams and Davis<sup>28</sup> showed that the inclusion of nonlinear effects (in the analysis of a surfactant-free thin liquid film) may be of particular significance for the predicted rupture time. Another type of interfacial instabilities is induced by the thermal fluctuations, these patterns are known as Bénard cells, after the pioneering experimental studies of Bénard. For many years this cellular instability was attributed to buoyancy-driven convection. Following Rayleigh, the phenomenon is now understood as a result of interfacial tension gradients. The coupling of the concentration and temperature instabilities was investigated by many authors.<sup>29–41</sup> They showed that the surface excess of adsorbed solute opposes the surface movement and delays or inhibits the appearance of instability. Experimental verification of these analyses was obtained by Imaishi *et al.*<sup>42</sup> The nonlinear stability of surfactant-free evaporating/condensing thin liquid films are discussed in Refs. 43–45. The authors proved that the evaporation and condensation lead to destabilization of the film. Hatzivramidis<sup>11</sup> investigated the influence of surfactant on the film stability in the case of an adsorption-controlled process.

In this paper we discuss the problem of linear stability of an evaporating wetting film in the presence of dissolved surfactant. The model of Burelbach *et al.*<sup>44</sup> is extended by taking into account the influence of interfacial viscosity, bulk and surface diffusivity of surfactant, and the surfactant Marangoni effect (see Sec. II). Appropriate dimensionless numbers are defined in such a way as to remain constant during the process of evaporation, when both the temperature and the concentration increase. In lubrication approximation we use the linearized theory to calculate the critical values of the film thickness and the wavelength of the perturbation. A strong influence of the initial surfactant concentration upon

the stability is observed for three different types of surfactant: ionic, nonionic, and high molecular weight (see Sec. IV).

## II. MATHEMATICAL FORMULATION

We consider an infinite thin viscous liquid layer, formed from a surfactant solution, which is sandwiched between an uniformly heated plate and the gaseous phase of the solvent vapor. The film is evaporating, so there is solvent mass flux, momentum transfer, and energy consumption at the vapor–liquid interface. Since the surfactant is nonvolatile, its concentration increases during the film thinning. As a consequence, the interfacial properties of the system will change. In accordance with the practical situation, the concentration of solutes will be considered to be small enough, such that the density and the bulk viscosity of the solution practically do not change with composition. A typical bulk concentration of high molecular weight surfactants is about  $10^{-2}$  kg/m<sup>3</sup>. Therefore the solution can be treated as an incompressible Newtonian fluid. Since the rupture thickness of films is of the order of 5–10 nm, the continuum theory of the liquid is applicable. We study the stability of films with initial thicknesses not greater than 20  $\mu$ m, therefore one can neglect gravity effects, but one has to take into account the macroscopic effects of intermolecular forces (van der Waals, electrostatic,<sup>9</sup> steric,<sup>9</sup> etc).

For an incompressible surfactant solution the transport equations of mass, momentum, energy, and surfactant in the liquid (film) phase are<sup>1,26</sup>

$$\nabla \cdot \mathbf{v} = 0, \quad (1a)$$

$$\frac{\partial \mathbf{v}}{\partial t} + \mathbf{v} \cdot \nabla \mathbf{v} = -\frac{1}{\rho} \nabla p + \frac{\eta}{\rho} \nabla^2 \mathbf{v}, \quad (1b)$$

$$\frac{\partial T}{\partial t} + \mathbf{v} \cdot \nabla T = \nabla \cdot (a \nabla T), \quad (1c)$$

$$\frac{\partial c}{\partial t} + \mathbf{v} \cdot \nabla c = \nabla \cdot (D \nabla c), \quad (1d)$$

where  $t$  is time,  $\nabla$  is the spatial gradient operator,  $\rho$ ,  $p$ , and  $T$  are the liquid density, pressure, and temperature,  $\mathbf{v}$  is the averaged mass liquid velocity,  $\eta$  is the dynamic viscosity,  $c$  is the bulk surfactant concentration,  $a$  is the thermal diffusivity of the solution, and  $D$  is the surfactant bulk diffusion coefficient.

On the heated film substrate,  $z=0$  (see Fig. 1), we assume constant temperature  $T_h$ , and no specific adsorption, which is equivalent to zero surfactant diffusion flux. So the boundary conditions at  $z=0$  are

$$\mathbf{v} = \mathbf{0}, \quad T = T_h, \quad \frac{\partial c}{\partial z} = 0. \quad (2)$$

The balances of mass and surfactant species at the film–vapor interface read<sup>26,44,46</sup> as

$$J = \rho(\mathbf{v} - \mathbf{u}_{ds}) \cdot \mathbf{n}, \quad (3a)$$

$$\frac{\partial \Gamma}{\partial t} + \nabla_s \cdot (\Gamma \mathbf{v}_s) - \nabla_s \cdot (D_s \nabla_s \Gamma) = [-D \nabla c + c(\mathbf{v} - \mathbf{u}_{ds})] \cdot \mathbf{n}. \quad (3b)$$

The following notation is used:  $\nabla_s$  is the surface gradient operator,<sup>26</sup>  $J$  is the mass flux due to the evaporation,  $\mathbf{u}_{ds}$  is the velocity of the dividing surface,  $\mathbf{n}$  is its normal vector pointing to the vapor phase (see Fig. 1),  $\Gamma$  is the adsorption,  $D_s$  is the interfacial diffusion coefficient, and  $\mathbf{v}_s$  is the continuous tangential component of the velocity at the interface. In the boundary condition for the surfactant concentration (3b) the effects of interfacial convection and diffusion and bulk diffusion are taken into account.

We consider the limiting case of small density, viscosity, and thermal conductivity of the gaseous phase as compared to the liquid (film) phase. Consequently, the stability is determined by the processes in the liquid phase.<sup>44</sup> In this limit the boundary conditions for the conservation of surface-excess linear momentum and energy reduce to

$$\eta[\nabla \mathbf{v} + (\nabla \mathbf{v})^T] \cdot \mathbf{n} = \nabla_s \cdot \mathbf{P}_s + \left( p + \Pi - p_v - \frac{J^2}{\rho_v} \right) \mathbf{n}, \quad (3c)$$

$$JL = -(\lambda \nabla T) \cdot \mathbf{n}, \quad (3d)$$

where  $L$  is the latent heat of vaporization,  $\lambda$  is the thermal conductivity of the liquid,  $\mathbf{P}_s$  is the surface stress tensor,  $\Pi$  is the disjoining pressure, and  $\rho_v$  and  $p_v$  are the vapor density and pressure, respectively. The superscript  $T$  in Eq. (3c) denotes conjugation.

There are many forces that influence the hydrodynamic instability of thin liquid films: capillary forces, tangential stresses caused by interfacial tension gradients induced by temperature and concentration inhomogeneities (Marangoni instability), buoyancy forces due to the temperature gradients (Bénard convection), and surface forces.<sup>9</sup> Whereas the first three are mainly responsible for triggering the instabilities, the molecular surface forces intervene increasingly in later stages of film evolution towards rupture. The influence of the van der Waals forces can be analyzed using the so-called body force model,<sup>10</sup> whereby their action is expressed in terms of the so-called disjoining pressure  $\Pi$  appearing in Eq. (3c):

$$\Pi = -\frac{A}{6\pi h^3}, \quad (4)$$

where  $A$  is the Hamaker constant.

If the interface of an equilibrium surfactant solution is disturbed the equilibrium will be restored either by adsorption from the bulk surfactant solution, or by surface convection, driven by the gradient of interfacial tension (elasticity of the interface) in interplay with a specific interfacial viscous friction (the so-called Boussinesq effect). A simple rheological model of the interfacial dynamics is provided by the linear Boussinesq–Scriven<sup>26</sup> constitutive law:

$$\mathbf{P}_s = [\sigma + (\eta_s^{\text{dil}} - \eta_s^{\text{sh}}) \nabla_s \cdot \mathbf{v}_s] \mathbf{I}_s + \eta_s^{\text{sh}} [(\nabla_s \mathbf{v}_s) \cdot \mathbf{I}_s + \mathbf{I}_s \cdot (\nabla_s \mathbf{v}_s)^T], \quad (5)$$

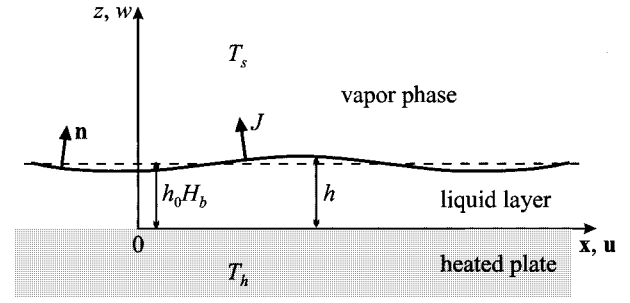


FIG. 1. The physical configuration describing an evaporating thin liquid film on a horizontal heated solid surface.

where  $\mathbf{I}_s$  is the surface unit operator. The physical parameters characterizing the surface are the interfacial tension  $\sigma$ , and the interfacial shear and dilatational viscosities,  $\eta_s^{\text{sh}}$  and  $\eta_s^{\text{dil}}$ , respectively.

In order to close the system of equations one has to add constitutive equations for the mass flux  $J$ . We will employ the simplification of the Hertz–Knudsen equation, given by Plesset<sup>47</sup> and widely used by many authors:

$$J = J_T(T_s - T_e), \quad \text{with } J_T = \text{const}, \quad \text{and } L = \text{const}, \quad (6)$$

where  $T_e$  is the equilibrium vapor temperature,  $T_s$  is the temperature of the fluid surface, and  $J_T$  and  $L$  depend on the solvent molecular weight and on the saturation temperature.

At the fluid interface there is a relation between the sub-surface bulk concentration  $c_s$  and the surfactant adsorption  $\Gamma$ , expressed by the adsorption isotherm. In addition, a surface equation of state connects the surface tension with the adsorption. For most of the surfactant solutions, below and close to the critical micellar concentration (CMC),  $c_{\text{CMC}}$ , one may use the Langmuir isotherm and the Frumkin equation of state,

$$\frac{\Gamma}{\Gamma_\infty} = \frac{c_s}{c_L + c_s}, \quad (7a)$$

$$\sigma = \sigma_p(T_s) + k_B T_s \Gamma_\infty \ln \left( 1 - \frac{\Gamma}{\Gamma_\infty} \right). \quad (7b)$$

In Eqs. (7a) and (7b)  $\Gamma_\infty$  is the saturation adsorption,  $c_L$  is a constant parameter of the adsorption isotherm, related to the energy of adsorption per molecule,  $\sigma_p(T_s)$  is the interfacial tension of the pure solvent at temperature  $T_s$ , and  $k_B$  is the Boltzmann constant. Although Eqs. (7a) and (7b) were originally derived for the special case of localized adsorption of noninteracting molecules, they can be successfully applied to various surfactants.<sup>48,49</sup> In a micellar solution the interfacial tension does not change significantly with increase of the surfactant concentration. In most of the practical systems the relative temperature difference  $T_h - T_e$  is not high and the parameters  $A$ ,  $\Gamma_\infty$ , and  $c_L$  change insignificantly.

### III. LUBRICATION APPROXIMATION AND SCALING OF THE MODEL

A sketch of an evaporating liquid film on a planar solid substrate is shown in Fig. 1. The vapor–liquid interface and

the substrate are located at  $z=h(\mathbf{x},t)$  and  $z=0$ , respectively, in the coordinate system with normal coordinate  $z$  and lateral coordinate  $\mathbf{x}$ . The lateral and normal velocity components are denoted by  $\mathbf{u}$  and  $w$ . It is known that short wave perturbations disappear faster than those of wavelengths longer than the film thickness, due to the higher viscous dissipation and capillary damping in the former case.<sup>10,12,43,44,46</sup> Therefore the long wave approximation will be applied to the solution of the problem in the sequel. The general frame for this approximation is given by small Reynolds number  $\rho h_0^2/(\eta t_d) \ll 1$ , large thermal Peclet number  $at_d/h_0^2 \gg 1$ , large diffusivity Peclet number  $Dt_d/h_0^2 \gg 1$ , and small slope of the interface  $h$ :  $(\nabla_s h)^2 \ll 1$ .<sup>44,46</sup> The characteristic time of film thinning is  $t_d$  [see Eq. (8) below] and  $h_0$  is the initial film thickness.

Burelbach *et al.*<sup>44</sup> showed that the viscous scales used by Williams and Davis<sup>43</sup> (which are appropriate to an isothermal layer) are not typical for our problem. A total rescaling of the governing system of equations, consistent with the lubrication theory, is needed. The scales used in Ref. 44 change by several orders of magnitude during the film thinning, they are included in a complicated way in the system of equations and are not convenient for our problem. In order to minimize the number of dimensionless parameters we will define the disappearance time  $t_d$ , and normal and lateral space dimensions,

$$t_d \equiv \frac{\rho h_0}{J_T \Delta T} \left( 1 + \frac{LJ_T h_0}{2\lambda} \right), \quad l \equiv \sqrt[4]{\frac{\sigma_0 t_d}{3\eta h_0}}, \quad t = t_d \tau, \quad (8)$$

$$\mathbf{x} = h_0 l \mathbf{X}, \quad z = h_0 Z,$$

where  $\tau$ ,  $Z$ , and  $\mathbf{X}$  are the dimensionless time and space coordinates,  $l \gg 1$  is the characteristic parameter of lateral wavelengths, and  $\sigma_0$  is the pure solvent interfacial tension at the initial time moment  $t=0$ . The dimensions of the pressure and the velocity can be found directly from the mass and momentum transport equations (1a) and (1b). The dimensionless film thickness  $H$ , pressure  $P$ , and normal and lateral velocity components,  $W$  and  $\mathbf{U}$ , are introduced as follows:

$$h = h_0 H, \quad p - p_v = \frac{12\eta l^2}{t_d} P, \quad w = \frac{h_0}{t_d} W, \quad \mathbf{u} = \frac{2lh_0}{t_d} \mathbf{U}. \quad (9)$$

In this approximation the leading-order solution of Eqs. (1a), (1b), and (1c) for the temperature and velocity distribution, obeying the boundary conditions (2) and (3d) and the constitutive equations (6), read as

$$\frac{T_h - T}{\Delta T} = \frac{Z}{\mathcal{K} + H}, \quad (10a)$$

$$\mathbf{U} = 3Z(Z - H)\nabla_{\parallel} P + \frac{Z}{H} \mathbf{U}_s, \quad (10b)$$

$$W = Z^2(3H - 2Z)\nabla_{\parallel}^2 P + 3Z^2\nabla_{\parallel} P \cdot \nabla_{\parallel} H - Z^2\nabla_{\parallel} \cdot \left( \frac{1}{H} \mathbf{U}_s \right), \quad (10c)$$

where  $\Delta T = T_h - T_e$  is the temperature difference,  $\nabla_{\parallel}$  is the dimensionless lateral projection of the spatial gradient opera-

tor  $\nabla$ ,  $\mathbf{U}_s$  is the lateral component of the dimensionless velocity at the interface, and the pressure  $P$  depends only on the time and the lateral coordinate. The deviation from equilibrium at the evaporating interface is measured by the dimensionless parameter  $\mathcal{K} \equiv \lambda/(LJ_T h_0)$ , appearing in Eq. (10a). A small deviation from equilibrium at the evaporating interface,  $\mathcal{K} \ll 1$ , corresponds to the quasiequilibrium limit, with constant interfacial temperature, equal to the equilibrium one.  $\mathcal{K} \gg 1$  corresponds to the case without evaporation in which the evaporation mass flux  $J$  is zero.

After substitution of the general solution (10) into the surface mass balance and the normal component of the surface-excess linear momentum equations (3a) and (3c), the leading-order equations for the shape of the dividing surface and for the pressure read as

$$\frac{\partial H}{\partial \tau} + \nabla_{\parallel} \cdot (H\mathbf{U}) = \nabla_{\parallel} \cdot (H^3 \nabla_{\parallel} P) - \frac{2\mathcal{K} + 1}{2(\mathcal{K} + H)}, \quad (11a)$$

$$P = \frac{\mathcal{E}}{4} \frac{\mathcal{K}^2}{(\mathcal{K} + H)^2} + \frac{\mathcal{W}}{6H^3} - \frac{1}{4} \left( 1 - \mathcal{S} \frac{\ln(1 - \mathcal{G})}{\ln(1 - \mathcal{S})} \right) \nabla_{\parallel}^2 H. \quad (11b)$$

From the lubrication approximation it follows that  $\nabla_{\parallel}$  is equal to the dimensionless form of the surface gradient operator  $\nabla_s$  (see Ref. 26). In Eq. (11b) the ratios of the van der Waals disjoining pressure, and of the loss of interfacial linear momentum due to evaporation, to the dynamic pressure in the film phase are represented, respectively, by the dimensionless numbers  $\mathcal{W}$  (called the van der Waals number below) and  $\mathcal{E}$ . We use the following definitions for these dimensionless parameters:  $\mathcal{W} \equiv Al^2/(4\pi\sigma_0 h_0^2)$ ;  $\mathcal{E} \equiv h_0(LJ_T \Delta T)^2/(\rho_v \sigma_0)$ . The last term in Eq. (11b) estimates the influence of the capillary pressure on the film stability. The dimensionless form of the Frumkin equation of state (7b) is substituted therein. The characteristic scale of the adsorption  $\Gamma$  is the respective value  $\Gamma_{\text{CMC}}$  at the critical micellar concentration  $c_{\text{CMC}}$ . The capacity of the interface is determined by the number  $\mathcal{G} \equiv \Gamma_{\text{CMC}}/\Gamma_{\infty}$ ; a measure of the slope of the interfacial tension versus the log of concentration is defined by  $\mathcal{S} \equiv -k_B \Gamma_{\infty} (T_h + T_e) \ln(1 - \mathcal{G})/(2\sigma_0)$ ; and the dimensionless adsorption at the interface is given by  $G = \Gamma/\Gamma_{\text{CMC}}$ . For all types of surfactant  $\mathcal{S}$  changes from 0.75 to 0.95 depending on the specific molecular interactions in the surfactant adsorption monolayer.<sup>48,49</sup> Only for very strong repulsion between the head groups of the surfactant molecules,  $\mathcal{S}$  reaches 0.75; the typical value of  $\mathcal{S}$  is about 0.9. The values of  $\mathcal{S}$  for water/air interfaces are in the range from 0.5 to 0.7, but for most surfactants it is about 0.5.

From the solution (10) and the lateral component of the surface-excess linear momentum equation (3c), one can obtain the leading-order equations for the dimensionless surface velocity,  $\mathbf{U}_s$ ,

$$H \nabla_{\parallel} P + \frac{1}{3H} \mathbf{U}_s = \frac{2\mathcal{M}\mathcal{K}}{3(\mathcal{K} + H)^2} \nabla_{\parallel} H - \frac{2\mathcal{A}}{3(1 - \mathcal{G})} \nabla_{\parallel} G + \frac{\mathcal{V}}{3} \nabla_{\parallel} \cdot (G \nabla_{\parallel} \mathbf{U}_s). \quad (11c)$$

TABLE I. Range of variations in the interfacial properties of surfactants at CMC and room temperature (typ.—typically).<sup>1,26,49,51</sup>

	Ionic	Nonionic	High molecular weight
$\sigma$ (N/m)	25–43 $\times 10^{-3}$ (typ. 32 $\times 10^{-3}$ )	27–48 $\times 10^{-3}$ (typ. 33 $\times 10^{-3}$ )	40–60 $\times 10^{-3}$ (typ. 50 $\times 10^{-3}$ )
$c_{\text{CMC}}$ (mol/m <sup>3</sup> )	0.5–50 (typ. 8)	0.01–2 (typ. 0.05)	1–100 $\times 10^{-3}$ kg/m <sup>3</sup> (typ. 0.01)
$\Gamma_{\text{CMC}}$ (mol/m <sup>2</sup> )	1–5 $\times 10^{-6}$ > (typ. 2 $\times 10^{-6}$ )	1–5 $\times 10^{-6}$ (typ. 2 $\times 10^{-6}$ )	1–6 $\times 10^{-6}$ kg/m <sup>2</sup> (typ. 3 $\times 10^{-6}$ )
$D$ (m <sup>2</sup> /s)	3–6 $\times 10^{-10}$ (typ. 5 $\times 10^{-10}$ )	1–5 $\times 10^{-10}$ (typ. 3 $\times 10^{-10}$ )	8 $\times 10^{-11}$ –5 $\times 10^{-10}$ (typ. 1 $\times 10^{-10}$ )
$D_s$ (m <sup>2</sup> /s)	1 $\times 10^{-11}$ –1 $\times 10^{-8}$	1 $\times 10^{-11}$ –1 $\times 10^{-8}$	1 $\times 10^{-11}$ –1 $\times 10^{-8}$
$\eta_s^m$ (mPa s)	1 $\times 10^{-8}$ –1 $\times 10^{-5}$ (typ. 1 $\times 10^{-6}$ )	1 $\times 10^{-7}$ –5 $\times 10^{-4}$ (typ. 1 $\times 10^{-6}$ )	1 $\times 10^{-4}$ –2 (typ. 5 $\times 10^{-3}$ )

The Marangoni effects due to interfacial thermal and adsorption gradients are included in the Marangoni and adsorption elasticity numbers:  $\mathcal{M} \equiv -3l^2 \Delta T (\partial \ln \sigma / \partial T) / 4$  and  $\mathcal{A} \equiv 3l^2 k_B (T_h + T_e) \Gamma_{\text{CMC}} / (8\sigma_0)$ . The classical Marangoni adsorption number, which is related to the Gibbs elasticity of the interface  $E_G = -\partial \sigma / \partial \ln \Gamma$ ,<sup>26,49</sup> is not convenient for the present investigation, because the Gibbs elasticity changes by several orders of magnitude with the increase of surfactant concentration from low values to CMC. In Eq. (11c) the Boussinesq–Scriven constitutive law (5) leads to coupling of the dilatational and shear interfacial viscosities in one surface viscosity, defined by  $\eta_s = \eta_s^{\text{dil}} + \eta_s^{\text{sh}}$ . Experimental results<sup>26</sup> obtained by surface waves methods show that the dependence of the interfacial viscosity on the surfactant concentration is analogous to that of the bulk viscosity of concentrated dispersions: the interfacial viscosity increases with concentration, in the range from zero up to concentrations slightly above CMC. For thin liquid films the interfacial viscous friction prevents the surface mobility around the CMC practically for all types of surfactant (see Sec. IV). Therefore, in Eq. (11c) the simple experimental linear relation between the interfacial viscosity and the adsorption,  $\eta_s = \eta_s^m \Gamma / \Gamma_{\text{CMC}}$ , is used, where  $\eta_s^m$  is the interfacial viscosity at CMC. The corresponding interfacial viscosity number is defined by  $\mathcal{V} \equiv \eta_s^m / (\eta l^2 h_0)$ .

In the lubrication approximation the solution of the diffusion equation (1d) is a sum of a uniform part,  $C(\mathbf{X}, \tau)$ , and a small perturbation,  $C_1(\mathbf{X}, Z, \tau) / l^2$ , where the dimensionless concentration is defined by scaling with  $c_{\text{CMC}}$ .  $C(\mathbf{X}, \tau)$  does not depend on the vertical coordinate  $Z$ , and is equal to the dimensionless subsurface concentration. The  $Z$  derivative of  $C_1(\mathbf{X}, Z, \tau) / l^2$  is comparable with the lateral and time derivatives of the subsurface concentration.<sup>46</sup> Then, after integrating the diffusion equation from 0 to  $H$ , using the boundary condition (2), the leading order of the surfactant mass flux on the right-hand side of the interfacial species transport equation (3b) becomes

$$\begin{aligned}
 & -\mathcal{B} \frac{\partial C_1}{\partial Z} + \mathcal{B} \nabla_{\parallel} H \cdot \nabla_{\parallel} C - C \frac{\partial H}{\partial \tau} \\
 & = -\frac{\partial}{\partial \tau} (HC) + \nabla_{\parallel} \cdot [\mathcal{B} H \nabla_{\parallel} C + (H^3 \nabla_{\parallel} P - H U_s) C].
 \end{aligned} \tag{12}$$

The bulk diffusion flux is scaled by using the characteristic time and length scales (8); the rescaled diffusivity Peclet number is  $\mathcal{B} \equiv D t_d / (l^2 h_0^2)$ . Using the general solution (10) and the surfactant mass flux expression (12), the interfacial species transport equation (3b) can be transformed to read as

$$\begin{aligned}
 & \frac{\partial}{\partial \tau} (G + \mathcal{L}HC) + \nabla_{\parallel} \cdot [2GU_s - \mathcal{B}(\mathcal{V} \nabla_{\parallel} G + \mathcal{L}H \nabla_{\parallel} C) \\
 & - \mathcal{L}HC(H^2 \nabla_{\parallel} P - U_s)] = 0,
 \end{aligned} \tag{13}$$

where  $\mathcal{V}$  is the ratio between the surface and bulk diffusion coefficients and the capacity of the liquid layer is determined by the number  $\mathcal{L} \equiv h_0 c_{\text{CMC}} / \Gamma_{\text{CMC}}$ .

In Table I the typical values of  $\Gamma_{\text{CMC}}$ ,  $c_{\text{CMC}}$ , the bulk and surface diffusion coefficients  $D$  and  $D_s$ , and  $\eta_s^m$  for nonionic, ionic, and high molecular weight surfactants are given. It is interesting to note that for a given film thickness  $\mathcal{L}$  can change by several orders of magnitude from one type of species to another; its magnitude increases with the increase of the initial film thickness. The values of  $\mathcal{A}$  are similar for the nonionic and ionic surfactants. For high molecular weight surfactants  $\mathcal{A}$  depend strongly on the chemical composition. It is seen that  $\eta_s^m$  changes by eight orders of magnitude. Experiments give results for the surface diffusion coefficient comparable to the bulk diffusion coefficient, which are independent of the surfactant concentration below and close to CMC.

One physical example of material properties is given by Burelbach *et al.*<sup>44</sup> for a dilute water solution, where  $T_e = 373$  K,  $\rho = 960$  kg/m<sup>3</sup>,  $\rho_v = 0.6$  kg/m<sup>3</sup>, kinematic viscosity  $\nu = 3.0 \times 10^{-7}$  m<sup>2</sup>/s,  $\lambda = 0.68$  J/(ms K),  $L = 2.3 \times 10^6$  J/kg,  $J_T = 3.56$  kg/(sm<sup>2</sup> K),  $A = 10^{-20}$  J,  $\sigma_0 = 5.89 \times 10^{-2}$  N/m, and  $\partial \sigma / \partial T = -1.8 \times 10^{-4}$  N/(mK). The dependencies of the parameters  $\mathcal{H}$  and  $\mathcal{E}$ ,  $\mathcal{W}$ , and  $\mathcal{M}$ ,  $\mathcal{V}$ , and  $\mathcal{B}$  and  $\mathcal{A}$  and  $\mathcal{L}$  on the initial film thickness, as calculated from these data, are given in Figs. 2(a)–2(d). The temperature difference was taken to be  $\Delta T = 10$  °C and the parameters characterizing the interface were taken from Table I with typical values for an ionic surfactant. It is seen that with an increase of the initial film thickness, the influence of the interfacial viscosity, bulk

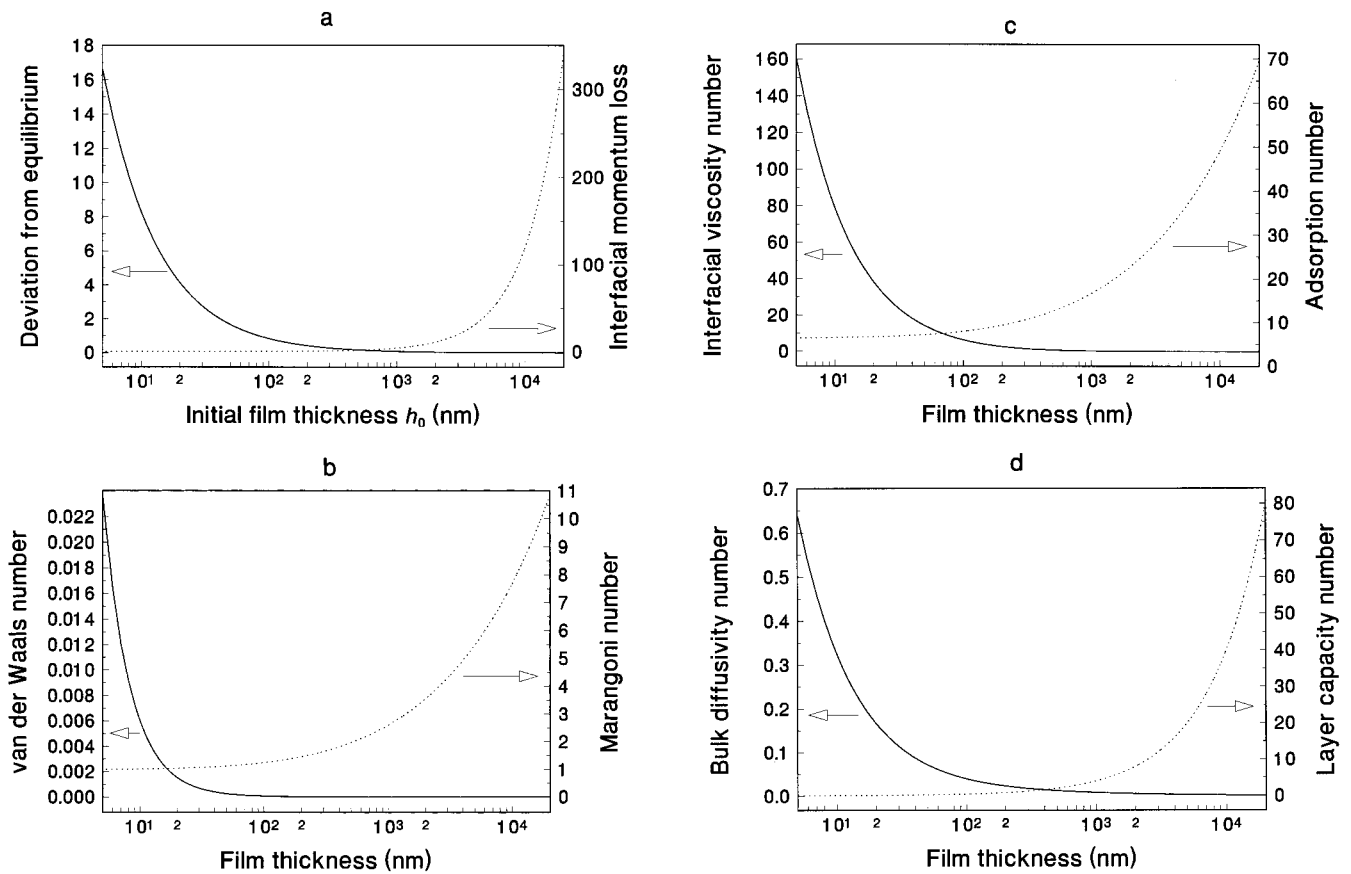


FIG. 2. The dependencies of the dimensionless parameters of ionic surfactant upon the initial film thickness for the temperature difference  $\Delta T = 10^\circ\text{C}$ : (a)  $\mathcal{H}$  and  $\mathcal{E}$ ; (b)  $\mathcal{W}$  and  $\mathcal{M}$ ; (c)  $\mathcal{V}$  and  $\mathcal{A}$ ; and (d)  $\mathcal{B}$  and  $\mathcal{L}$ .

diffusivity, and van der Waals disjoining pressure decrease. The decrease of the evaporation parameter,  $\mathcal{H}$ , leads to more pronounced thermal Marangoni and adsorption effects, to an increase of the interfacial linear momentum loss and capacity. If all other parameters are kept constant and only the type of surfactant is changed from ionic to high molecular weight, then  $\mathcal{V}$  increases and  $\mathcal{L}$  decreases by several orders of magnitude. The parameters  $\mathcal{H}$  and  $\mathcal{L}$  do not depend on the temperature difference; the others are connected with  $\Delta T$  as follows:  $\mathcal{W} \propto (\Delta T)^{-1/2}$ ,  $\mathcal{E} \propto (\Delta T)^{3/2}$ ,  $\mathcal{M} \propto (\Delta T)^{1/2}$ ,  $\mathcal{V} \propto (\Delta T)^{1/2}$ ,  $\mathcal{A} \propto (\Delta T)^{-1/2}$ , and  $\mathcal{B} \propto (\Delta T)^{-1/2}$ . Therefore, a change of the temperature difference influences significantly the interfacial linear momentum loss,  $\mathcal{E}$ , due to the evaporation.

It should be noted that the parameters  $\mathcal{E}$  and  $\mathcal{M}$  change only slightly for a wide range of variation of the initial film thickness. In contrast, the so-called rescaling parameters used in Ref. 44 change by several orders of magnitude. Moreover, the relationships (8.3b) and (9.3) of Ref. 44 are erroneous, which causes a decrease of the respective values from  $10^5$  to  $10^2$  and makes the physical conclusions there not exact. Another case of practical importance is discussed in Ref. 11 for enhanced oil recovery operations. For this quite different system the corresponding dimensionless parameters fall within the range studied by us. The values can be found in Fig. 2.

Our model based on Eqs. (11) and (13) extends that used

by Burelbach *et al.*<sup>44</sup> for the nonlinear stability analysis of an evaporating/condensing liquid film, by including interfacial viscosity, elasticity, and diffusivity effects due to the presence of a surfactant. The linear analysis of Hatzivramidis<sup>11</sup> is applicable only for barrier-controlled kinetics of surfactant adsorption. In the latter case the interfacial rheology is of crucial importance for the surface mobility. However, the effects due to surface diffusion and surface viscosity were not taken into account by Hatzivramidis.<sup>11</sup> The linear model of Ji and Setterwall<sup>50</sup> for the influence of diffusion-controlled kinetics of adsorption upon the stability of vertical falling liquid film is closer to the reality for large thickness, where the evaporation, interfacial viscosity and diffusivity, and disjoining pressure effects might be not so well pronounced.

#### IV. NONPERTURBED STATE AND LINEAR ANALYSIS

The nonperturbed state is assumed to be static,  $\mathbf{U}_s = \mathbf{0}$ , with a flat evaporating interface. We denote the nonperturbed quantities by a subscript  $b$ . Burelbach *et al.*<sup>44</sup> report the resulting leading-order basic-state solution for the film thickness, pressure, and mass flux. We will use the time dependence of the dimensionless film thickness and mass flux in the form

$$H_b = [\mathcal{H}^2 + (1 + 2\mathcal{H})(1 - \tau)]^{1/2} - \mathcal{H},$$

$$\frac{J_b}{J_T \Delta T} = \frac{\mathcal{H}}{[\mathcal{H}^2 + (1 + 2\mathcal{H})(1 - \tau)]^{1/2}}. \quad (14)$$

The time for which zero film thickness would be achieved as a result of thinning (without any fluctuations) is called in the literature the disappearance time,  $t_d$ ; it corresponds to  $\tau = 1$ . As a rule, because of instabilities in the evaporating thin liquid film, the latter ruptures at times shorter than  $t_d$ . The increasing of the evaporation number  $\mathcal{H}$  decreases the disappearance velocity and the film thickness changes more slowly with time. The mass flux increases with time, which is not very pronounced initially, but with decreasing film thickness,  $H_b$ , the intensity of evaporation rises significantly.

From Eq. (13) the nonperturbed state for the adsorption  $G_b$  and bulk concentration  $C_b$  ( $G_b + \mathcal{L}H_bC_b = G_0 + \mathcal{L}C_0$ ) is equivalent to the conservation of the total surfactant mass in the layer. The initial adsorption  $G_0$  and concentration  $C_0$  correspond to the adsorption  $\Gamma_0$  and bulk concentration  $c_0$  at  $t=0$ . For small initial amounts of adsorbed species, when  $G_0 + \mathcal{L}C_0 \leq 1$ , at vanishing film thickness  $H_b=0$  the adsorption approaches values  $G_b \rightarrow G_0 + \mathcal{L}C_0$  smaller than that at the CMC. In this case there is no micelle formation in the solution. From the Langmuir isotherm (7a) one may deduce the time dependence of the adsorption in the nonperturbed film,

$$G_b = \frac{1}{2} \left[ F + G_0 - \left( (F - G_0)^2 - 4 \frac{\mathcal{L}G_0}{\mathcal{L}} (1 - \mathcal{F}) \times (1 - H_b) \right)^{1/2} \right], \quad C_b = \frac{(1 - \mathcal{F})G_b}{1 - \mathcal{F}G_b},$$

$$F \equiv \frac{1}{\mathcal{L}} + \frac{\mathcal{L}(1 - \mathcal{F})G_0}{1 - \mathcal{F}G_0} \left( 1 + \frac{1 - \mathcal{F}G_0}{\mathcal{F}G_0} H_b \right). \quad (15)$$

In the opposite case of large concentrations,  $G_0 + \mathcal{L}C_0 > 1$ , we can define a thickness  $H_{\text{CMC}} = C_0 + (G_0 - 1)/\mathcal{L}$  at which micelles appear in the solution. For thicknesses  $H_b$  larger than  $H_{\text{CMC}}$ , the adsorption increases due to fast diffusion and reaches its final value at CMC. For smaller thicknesses  $H_b < H_{\text{CMC}}$ , the adsorption has a constant value and the quantity of surfactant incorporated in the micelles is  $C_b - 1 = H_{\text{CMC}}/H_b - 1$ . The time dependence of the adsorption is shown in Fig. 3 for different initial values, and for different layer capacities  $\mathcal{L}$ . Increasing of the layer capacity leads to faster interfacial saturation. This effect is more pronounced for higher initial concentration values (corresponding to greater values of  $G_0$ ).

For the linear analysis of the system (11) and (13), we introduce a small perturbation of pressure, interfacial velocity and shape, adsorption, and surfactant concentration with respect to the nonperturbed state (14)–(15). The perturbations are in the form of surface waves with dimensionless wave vector  $\mathbf{k}$  and lateral wave functions  $F_0 = \cos(\mathbf{k} \cdot \mathbf{X})$  and  $F_1 = \sin(\mathbf{k} \cdot \mathbf{X})$ . Then the perturbed physical parameters of the problem can be put in the form

$$H = H_b(1 + H_f F_0), \quad P = P_b + P_f F_0, \quad \mathbf{U}_s = \mathbf{U}_f F_1, \quad (16a)$$

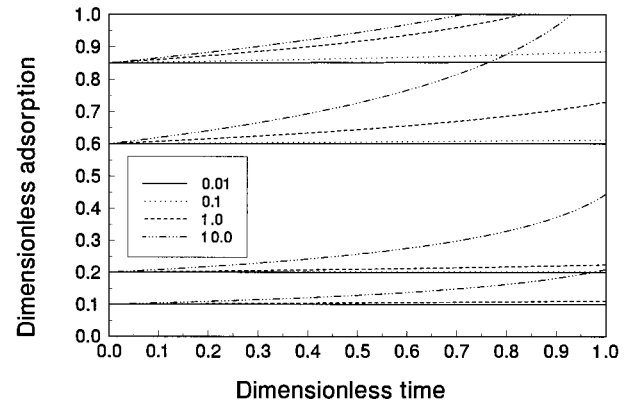


FIG. 3. The dimensionless nonperturbed adsorption  $G_b$  versus time, for different initial adsorption  $G_0=0.1, 0.2, 0.6$ , and  $0.85$ , and different surfactant layer capacity  $\mathcal{L}=0.01, 0.1, 1.0$ , and  $10.0$ . The degree of nonequilibrium is  $\mathcal{H}=1.5$ .

$$G = G_b + G_f F_0, \quad C = C_b + C_f F_0, \quad (16b)$$

where the perturbation amplitudes are given with subscript  $f$ ; they depend only on the dimensionless time  $\tau$ . The perturbation amplitude  $H_f$  of the surface shape is defined relative to the film thickness  $H_b$  of the nonperturbed state, which decreases with time due to evaporation.

The linearized form of normal (11b) and tangential (11c) projections of the vectorial boundary conditions lead to explicit relations connecting the pressure and velocity amplitudes with the shape fluctuation and with the total surfactant fluctuation amplitude, defined by  $S_f \equiv G_f + \mathcal{L}H_b C_f$ . These expressions read as

$$P_f = p_h H_f, \quad p_h \equiv -\frac{\mathcal{E}\mathcal{H}^2 H_b}{2(\mathcal{H} + H_b)^3} - \frac{\mathcal{W}}{2H_b^3} + \frac{k^2 H_b}{4} \times \left( 1 - \mathcal{F} \frac{\ln(1 - \mathcal{F}G_b)}{\ln(1 - \mathcal{F})} \right), \quad (17a)$$

$$\mathbf{k} \cdot \mathbf{U}_f = u_h H_f + u_s S_f, \quad (17b)$$

$$u_h \equiv \frac{k^2}{1 + f_v} \left( 3p_h H_b^2 - \frac{2\mathcal{H}\mathcal{M}H_b^2}{(\mathcal{H} + H_b)^2} \right),$$

$$u_s \equiv \frac{2k^2 \mathcal{A}H_b}{(1 + f_v)(1 + f_s)(1 - \mathcal{F}G_b)}, \quad (17c)$$

where the surfactant factor  $f_s \equiv \mathcal{L}H_b(1 - \mathcal{F})/(1 - \mathcal{F}G_b)^2$  is calculated using the dimensionless form of the Langmuir isotherm (7a),  $f_v \equiv k^2 \mathcal{F}G_b H_b$  is the interfacial viscosity factor, and  $k^2 = \mathbf{k} \cdot \mathbf{k}$  is the squared modulus of the wave vector. The influence of the layer capacity on the wave amplitudes is measured by  $f_s$  and the suppressing effect of the interfacial viscosity on the interfacial mobility is included in  $f_v$ . The substitution of the perturbation state (16) into the surface mass and species transport equations, (11a) and (13), and the subsequent linearization of the resulting system leads to the linear equations for the surface shape and the surfactant perturbation amplitudes:

$$\frac{dH_f}{d\tau} = a_{11}H_f + a_{12}S_f, \quad \frac{dS_f}{d\tau} = a_{21}H_f + a_{22}S_f. \quad (18)$$

The coefficients of the problem (18) depend on time,  $\tau$ , and wave number,  $k$ , in the following complicated manner:

$$a_{11} = \frac{(2\mathcal{H}+1)(\mathcal{H}+2H_b)}{2H_b(\mathcal{H}+H_b)^2} - u_h - k^2 H_b^2 p_h, \quad a_{12} = -u_s, \quad (19a)$$

$$a_{21} = \frac{dG_b}{d\tau} - \mathcal{L}C_b \frac{(2\mathcal{H}+1)(\mathcal{H}+2H_b)}{2(\mathcal{H}+H_b)^2} - 2G_b u_h, \quad (19b)$$

$$a_{22} = -2G_b u_s - k^2 \mathcal{B} \frac{\mathcal{I} + f_s}{1 + f_s}.$$

For pure liquid, Eqs. (17)–(19) reduce to those of Burelbach *et al.*<sup>44</sup> If the effects of the bulk and interfacial diffusivities and interfacial viscosities are neglected, one recovers the stability analysis of Ref. 11. If the evaporation effect is negligible, the coefficients of the system (18) become independent of time and the linear analysis gives results that have been widely discussed in the literature (see Refs. 8, 10, 24–26, 38).

The time dependence of the nonperturbed state affects the wavelength at which the fluctuation has a maximum increment at a given time moment. Following the idea of linear stability analysis of draining thin liquid films,<sup>18,19</sup> we will define the critical film rupture time  $\tau_c$  for an initial amplitude  $H_f(0)$ . When the amplitude of the perturbation with a given wave number  $k$  is equal to 1, the film will rupture, and this moment defines the rupture time  $\tau_r$ . The minimum of  $\tau_r$  for all possible wave numbers  $k$  gives the critical film rupture time  $\tau_c$ . The corresponding dimensionless thickness and wave number are called here the critical film thickness  $H_c$  and wave number  $k_c$ . In the special limiting case of tangentially immobile surfaces and pure liquid phase the problem (17)–(19) has an analytical solution (see Secs. IV A and IV B). The influence of surfactant concentration is investigated numerically in Sec. IV C.

### A. Tangentially immobile interfaces

When the surfactant concentration is close to or above the CMC, the surface elasticity and viscosity are high enough to prevent the tangential mobility of the interface and the surface velocity is zero,  $\mathbf{U}_f = \mathbf{0}$  (see Refs. 25 and 26). In Sec. IV C we prove that practically this assumption is valid for all types of surfactant; only for high-temperature difference, thick films, and lowest values of the interfacial viscosity at the CMC known from the literature,<sup>51</sup> this assumption can be incorrect [see the discussion of Fig. 7(b)]. In the case of tangential immobility,  $G_b = 1$  and the exact solution for  $H_f$  is shown in the Appendix. From the condition for an extremum of  $\tau_r$ ,  $d\tau_r/dk = 0$ , one can derive a system of transcendental equations for the calculation of the critical film thickness  $H_c$  and the corresponding wave number  $k_c$ . This result is

$$\ln\left(\frac{H_f(0)}{H_c}\right) + \ln\left(\frac{\mathcal{H}+1}{\mathcal{H}+H_c}\right) + \frac{1-\mathcal{I}}{2(2\mathcal{H}+1)} \left( \frac{\mathcal{H}}{4} (1-H_c^4) + \frac{1}{5} (1-H_c^5) \right) k_c^4 = 0, \quad (20a)$$

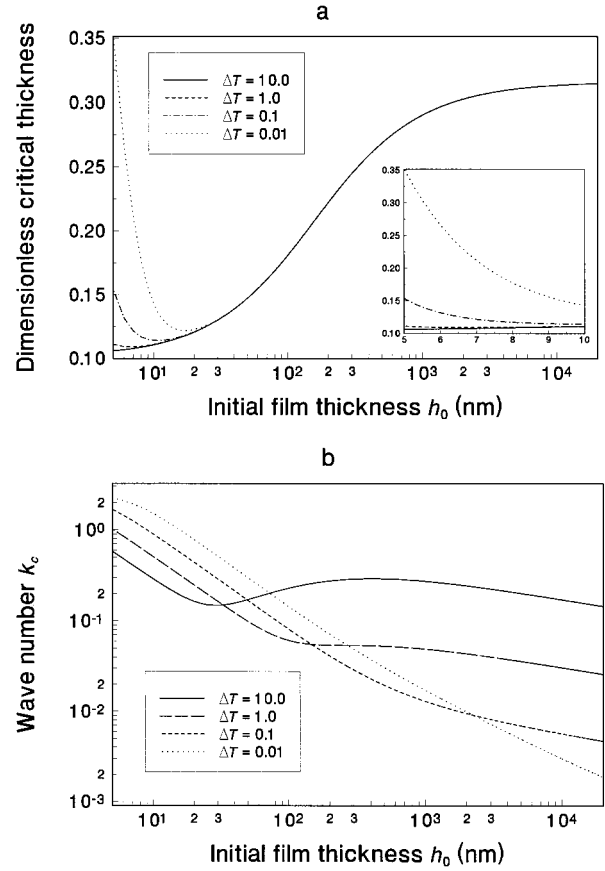


FIG. 4. Dependence of the critical parameters on the initial film thickness  $h_0$  for tangentially immobile interfaces: (a) dimensionless critical thickness  $H_c$  at  $\Delta T = 0.01$  °C, 0.1 °C, 1 °C, and 10 °C, and (b) critical wave number  $k_c$  and  $\Delta T = 0.01$  °C, 0.1 °C, 1 °C, and 10 °C.

$$3\mathcal{E}\mathcal{H}^4 \ln\left(\frac{\mathcal{H}+1}{\mathcal{H}+H_c}\right) + \mathcal{E}\mathcal{H}^2 \left( \frac{1-H_c^2}{2} - 2\mathcal{H}(1-H_c) - \frac{\mathcal{H}^3(1-H_c)}{(\mathcal{H}+1)(\mathcal{H}+H_c)} \right) + \mathcal{W}\mathcal{H} \ln\left(\frac{1}{H_c}\right) + \mathcal{W}(1-H_c) - (1-\mathcal{I}) \left( \frac{\mathcal{H}}{4} (1-H_c^4) + \frac{1}{5} (1-H_c^5) \right) k_c^2 = 0. \quad (20b)$$

In order to investigate the dependence of the critical parameters on the initial film thickness  $h_0$ , we computed numerically the solution of Eq. (20) for parameters described in Sec. III. The results for the dimensionless critical thickness  $H_c$  and wave number  $k_c$  are presented in Fig. 4. The initial fluctuation amplitude  $H_f(0)$  is chosen to be 0.1; the same initial condition was used in Refs. 28 and 44. It is seen from Fig. 4(a) that at an initial film thickness larger than 30 nm the dimensionless critical thickness does not depend on the temperature difference but increases about two times with the increase of  $h_0$  up to 20  $\mu\text{m}$ . For  $0.01 \leq \Delta T \leq 10$  °C the van der Waals attraction does not influence the film stability ( $\mathcal{W} \propto \Delta T^{-1/2}$ ). The increase of  $H_c$  in the interval above  $h_0 = 30$  nm is a result of the interplay of the pure evaporating instabilities. For smaller initial film thickness,  $h_0$ , the van der Waals disjoining pressure has a significant effect on the film stability for small temperature differences. In this case



the intensive evaporation suppresses the destabilizing effect of surface forces: when  $\Delta T = 10^\circ\text{C}$  their influence is negligible for all values of the initial thickness  $h_0$ . The decrease of the temperature difference results in more than three times higher critical thickness at  $\Delta T = 0.01^\circ\text{C}$ . We find also that for all used values of  $h_0$  and  $\Delta T$  the influence of the interfacial momentum loss (due to the evaporation) on the critical parameters is extremely small and can be disregarded. The effect of the evaporation and van der Waals attraction on the critical wavelength is well pronounced [see Fig. 4(b)]. For large initial film thickness, where the surface forces are not operative, the decreasing of the temperature difference  $\Delta T$  leads to longer critical waves, at constant  $H_c$ . The opposite behavior is manifested for thicknesses below 50 nm: the smaller the  $\Delta T$ , the larger the wave number  $k_c$ , and the longer the critical wavelength.

## B. Surfactant-free film

For surfactant-free film the interfacial velocity depends only on the pressure distribution; then the governing system (17)–(19) reduces to one differential equation, which has an exact solution given in the Appendix. The condition for an extremum time of rupture,  $d\tau_r/dk = 0$ , leads to the following system of transcendental equations for the calculation of the critical film thickness  $H_c$  and wave number  $k_c$ :

$$\ln\left(\frac{H_f(0)}{H_c}\right) + \ln\left(\frac{\mathcal{H}+1}{\mathcal{H}+H_c}\right) + \frac{2}{2\mathcal{H}+1} \left(\frac{\mathcal{H}}{4} (1-H_c^4) + \frac{1}{5} (1-H_c^5)\right) k_c^4 = 0, \quad (21a)$$

$$\begin{aligned} (3\mathcal{E}\mathcal{H}^4 + \mathcal{M}\mathcal{H}^3) \ln\left(\frac{\mathcal{H}+1}{\mathcal{H}+H_c}\right) + \mathcal{E}\mathcal{H}^2 \left(\frac{1-H_c^2}{2} - 2\mathcal{H}(1-H_c) - \frac{\mathcal{H}^3(1-H_c)}{(\mathcal{H}+1)(\mathcal{H}+H_c)}\right) + \mathcal{W}\mathcal{H} \ln\left(\frac{1}{H_c}\right) \\ + \mathcal{W}(1-H_c) + \mathcal{M}\mathcal{H} \left(\frac{1-H_c^2}{2} - \mathcal{H}(1-H_c)\right) \\ - \left[\frac{\mathcal{H}}{4} (1-H_c^4) + \frac{1}{5} (1-H_c^5)\right] k_c^2 = 0. \end{aligned} \quad (21b)$$

There are two factors acting in opposite directions. The higher surface tension (as compared to the case with surfactant) stabilizes the film. Due to the motion of the interface and the lateral temperature gradients, the thermal Marangoni term in Eq. (21b) increases the critical wave number and decreases the critical film thickness. Hence the thermal Marangoni effect destabilizes the evaporating film. The quantitative explanation of these effects is presented in Fig. 5, where the critical parameters are plotted as functions of the initial film thickness for temperature differences  $\Delta T = 0.01^\circ\text{C}$ ,  $0.1^\circ\text{C}$ ,  $1^\circ\text{C}$ , and  $10^\circ\text{C}$ , at the same dimensionless evaporation numbers as in Fig. 2. In contrast with the case of tangentially immobile surfaces, for large initial film

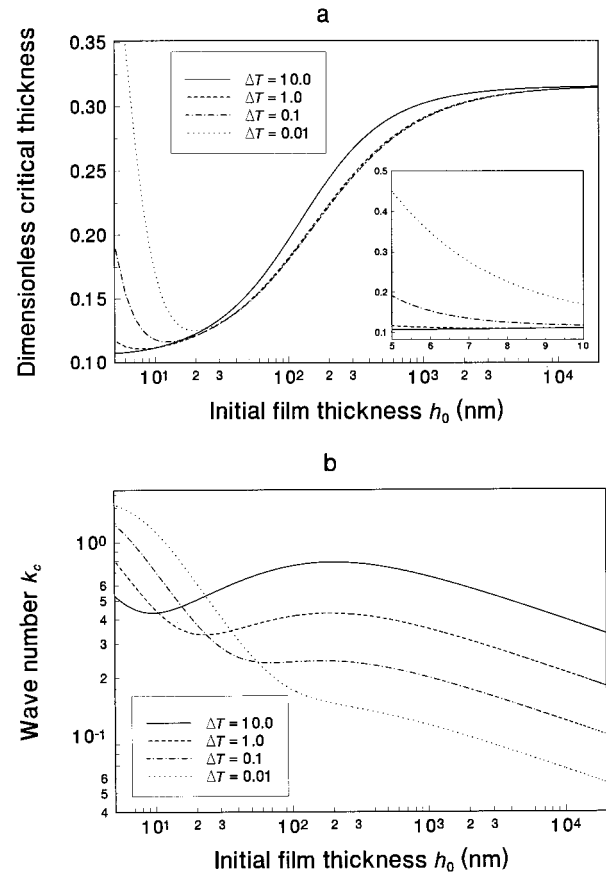


FIG. 5. Dependence of the critical parameters on the initial film thickness  $h_0$  for temperature differences  $\Delta T = 0.01^\circ\text{C}$ ,  $0.1^\circ\text{C}$ ,  $1^\circ\text{C}$  and  $10^\circ\text{C}$ , for surfactant-free film: (a) dimensionless critical thickness  $H_c$ , and (b) critical wave number  $k_c$ .

thickness and large enough temperature difference, the thermal Marangoni effect produces additional destabilization of the film, as  $H_c$  increases.

For smaller  $h_0$ , where the van der Waals attraction plays an important role, the higher interfacial mobility leads to increase of the critical thickness. The two times higher surface tension cannot prevent the Marangoni, van der Waals, and evaporation instabilities, whose coupling leads to smaller critical film lifetime  $\tau_c$  as compared to the case of high surfactant concentration. The comparison between Fig. 4(a) and Fig. 5(a) shows that for  $h_0 = 5$  nm and  $\Delta T = 0.01^\circ\text{C}$  the critical thickness increases from about 0.35 up to 0.45. The conclusions of Sec. IV A that the high-temperature difference makes the processes of film disappearing and instability comparable to each other is confirmed also for the pure film liquid phase. The critical wave number depicted in Fig. 5(b) for  $\Delta T = 10^\circ\text{C}$  has a different behavior when compared to its dependence shown in Fig. 4(b). At small distances the longer waves destabilize the film in contrast to the case of large distances, where the critical wavelength is smaller. With decreasing of the temperature difference this tendency reverts to the opposite and the wave numbers decrease monotonically with the increase of the initial film thickness.

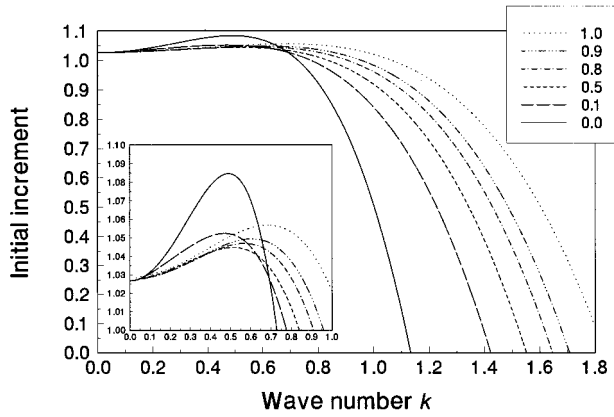


FIG. 6. Initial increment  $\omega$  versus the wave number  $k$  for typical parameters of an ionic surfactant and different initial adsorption  $G_0=0, 0.1, 0.5, 0.8, 0.9$  and  $1$ . The initial film thickness is  $h_0=5$  nm and the temperature difference is  $\Delta T=0.1$  °C.

### C. Influence of surfactant concentration

For the solution of the linear system (18) we need additionally an initial condition for the total surfactant fluctuation amplitude  $S_f(0)$ . For that purpose we performed an asymptotic analysis for  $\tau \rightarrow 0$ . In this limit the fluctuation amplitudes are proportional to the exponential time factor  $\exp(\omega\tau)$ , where  $\omega$  is the initial increment/decrement. After a substitution of the exponential factor into (18) the latter transforms into a dispersion relation for determining  $\omega$ . There are two solutions, but we chose the greater one  $\omega_r$ . The cutoff initial wave number  $k_0$  corresponds to  $\omega_r=0$ . Then the initially unstable waves ( $\omega_r > 0$ ) have the wave numbers such that  $0 < k^2 < k_0^2$ , and for each  $k$  the initial condition leading to faster film rupture is  $S_f(0) = a_{21}(0)H_f(0)/[\omega_r - a_{22}(0)]$ . Figure 6 shows typical curves  $\omega_r(k)$ . The computations were performed for the ionic surfactant (see Table I) at  $h_0=5$  nm and  $\Delta T=0.1$  °C. The initial adsorption takes values  $G_0=0, 0.1, 0.5, 0.8, 0.9$ , and  $1$ . The plots show a growing range of initially unstable waves with the increase of surfactant concentration. The very long waves ( $k \ll 1$ ) are unstable due to the effect of evaporation: in the thinner part of the film the interfacial temperature is higher, which increases the rate of evaporation, and this results in a faster decrease of the film thickness. At a wide range of wave numbers  $k^2 < 1$ , the initial increment undergoes little change. The surfactant concentration influences the maximum of the initial increment (see the inset in Fig. 6). At small adsorption its increase leads to a decrease of  $\omega_r$ . In contrast, at adsorption larger than about 0.5 the increase of surfactant concentration plays an initially destabilizing role. This fact is not discussed in the literature (see Refs. 10, 11, 18, 24, and 50).

In order to obtain a precise numerical solution of the problem (18), we used the Runge–Kutta fourth-order numerical scheme with time step  $1 \times 10^{-4}$ . For all cases the critical wave number  $k_c$  was computed to be smaller than the initial wave number at which the initial increment  $\omega_r$  has a maximum. The influence of surfactant type and concentration on the critical film thickness is illustrated in Fig. 7 for the limiting cases of small and large initial film thickness and

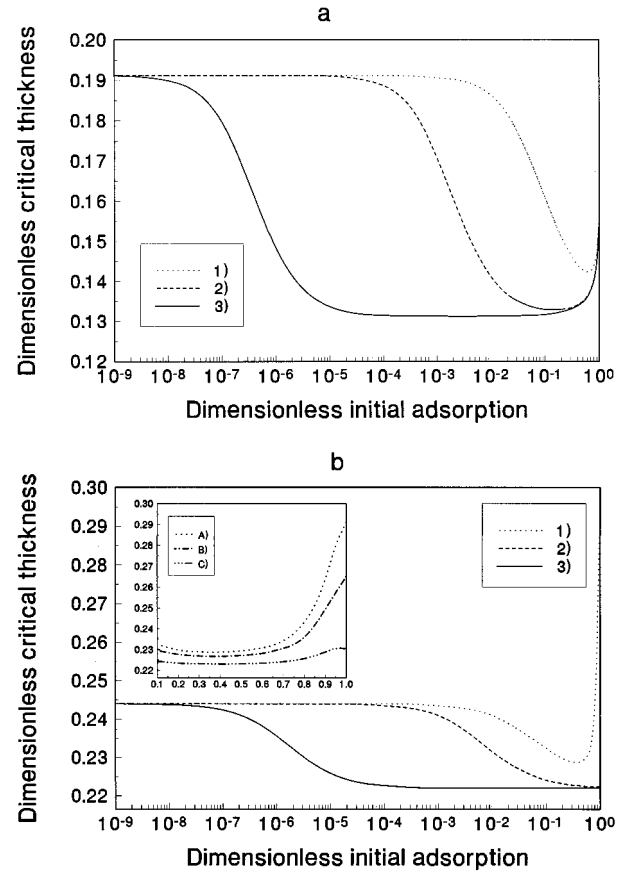


FIG. 7. Critical film thickness  $H_c$  versus dimensionless initial adsorption  $G_0$  for typical parameters of ionic (1), nonionic (2), and high molecular weight surfactant (3): (a)  $h_0=5$  nm and  $\Delta T=0.1$  °C, and (b)  $h_0=200$  nm and  $\Delta T=10$  °C [in the inset the interfacial viscosity for the ionic surfactant is, respectively, (a)  $\eta_s^m = 1 \times 10^{-8}$  mPa s, (b)  $\eta_s^m = 1 \times 10^{-7}$  mPa s, and (c)  $\eta_s^m = 1 \times 10^{-6}$  mPa s].

the temperature difference. In Fig. 7(a) the parameter values are  $h_0=5$  nm and  $\Delta T=0.1$  °C. Curves 1, 2, and 3 are plotted with typical parameter values for ionic, nonionic, and high molecular weight surfactant, respectively. For all types of surfactant the increase of its concentration causes a decrease of the critical thickness. The surfactant stabilizing effect is most pronounced for the smallest values of the critical thickness. The physical explanation of this behavior is connected with the faster growth of the interfacial elasticity and viscosity in comparison with the not so pronounced decrease of the interfacial tension. In the region where the critical thickness levels off, the interface is practically tangentially immobile and the additional increasing of the surfactant concentration cannot affect the surface dynamics; it only decreases the surface tension that plays a destabilizing role. Therefore, the dynamic interfacial characteristics [Gibbs elasticity, capacity of the layer, interfacial viscosity, diffusion relaxation time  $(\partial\Gamma/\partial c)^2/D$ , etc.] are more important than the change of the surface tension for small concentration. The efficiency of the ionic surfactant (see curve 1) is much smaller than that of the two other types. Its lower elasticity and interfacial viscosity and higher layer capacity are not sufficient in all concentration ranges to produce interfacial solidification. The stabilizing effect of the high mo-

lecular weight surfactant is well pronounced in the range of large concentrations. A small amount of such a surfactant practically makes the interface immobile. When the film thickness and the temperature difference are large enough, the faster evaporation suppresses the effect of surface tension changes for concentrations close to CMC. This is illustrated in Fig. 7(b), where the corresponding initial film thickness was 200 nm and temperature difference was 10 °C. Curves 3 and 2 are plotted with typical parameter values for a high molecular weight and nonionic surfactant, respectively, and curve 1 corresponds to typical parameters for an ionic surfactant, with low values of the interfacial viscosity<sup>51</sup> (see Table I). One sees the similar behavior of the films stabilized by a nonionic and high molecular weight surfactant, as in Fig. 7(a). After reaching a minimum, the critical thickness does not change anymore. For illustrating the interfacial viscosity effect, we varied its value for the ionic surfactant. The corresponding results are shown in the inset in Fig. 7(b), where (a)  $\eta_s^m = 1 \times 10^{-8}$  mPa s; (b)  $\eta_s^m = 1 \times 10^{-7}$  mPa s, and (c)  $\eta_s^m = 1 \times 10^{-6}$  mPa s; the latter is a typical value for the ionic surfactant. The significant effect of the interfacial viscosity at large concentrations is visible. The critical thickness decreases from 0.291 to 0.224 only due to the increase of the interfacial viscosity, keeping all other parameters constant.

## V. CONCLUSIONS

The theoretical model developed above for computing the evolution of a thin liquid film on a horizontal heated solid substrate makes it possible to investigate how the film stability is affected by the evaporation and the surfactant dissolved in the film phase. The theory is applicable for a small Reynolds number, large thermal and diffusion Peclet numbers, and a small slope of the interface. The influence of the van der Waals disjoining pressure is taken into account, as an example of the intermolecular force. In the limiting case of small vapor density, viscosity, and thermal conductivity, the vapor phase decouples and the stability problem for the liquid phase is solved separately. In this paper the linear analysis leads to a minimization problem for numerical computation of the critical thickness and the critical lateral wavelength. The nonlinear analysis is a subject of future work.

The dimensionless numbers appearing in the problem are classified in two groups: the first one is connected with evaporation and the Marangoni effect, and the second one gives the influence of the surfactant on the stability. For a real physical system, the influence of the interfacial viscosity, bulk diffusivity, deviation from equilibrium, and van der Waals forces decreases with an increase of the initial film thickness. Moreover, the role of the interfacial mass loss, the temperature and concentration Marangoni effects, and the surfactant layer capacity becomes more important.

In the case of a large amount of surfactant, the interface liquid–vapor is tangentially immobile. For initial film thicknesses smaller than 30 nm the influence of the van der Waals attraction leads to an increase of the dimensionless critical thickness for small temperature differences  $\Delta T$ . The impact

of the van der Waals forces is suppressed when the deviation from equilibrium,  $\mathcal{N}$ , is greater for larger temperature differences  $\Delta T$ . For initial film thicknesses larger than 30 nm, and for  $0.01 \text{ °C} \leq \Delta T \leq 10 \text{ °C}$ , only the evaporation influences the instability. For the surfactant-free liquid phase the interfacial tension is larger, which stabilizes the film, but the interface is mobile and the thermal Marangoni effect produces additional destabilization. The higher surface tension cannot prevent the various kinds of instabilities, which altogether lead to a smaller critical lifetime. Moreover, the temperature difference  $\Delta T$  influences the critical film thickness,  $H_c$ , up to an initial thickness of 20  $\mu\text{m}$ ; see Figs. 4 and 5. For a given initial film thickness and temperature difference the increasing of initial surfactant concentration stabilizes the film, but this trend is observed only up to the moment of reaching tangential immobility of the interface due to the increase of its interfacial viscosity and elasticity; see Fig. 7. After that, the additional increase of surfactant concentration (approaching the CMC) leads only to a decrease of interfacial tension, and this lowers the film stability. The latter effect does not comply with the commonly accepted rule that the increase of surfactant concentration always leads to higher stability. The efficiency of the ionic surfactants is much smaller than that of nonionic and high molecular weight surfactants, because the immobilization of the interface occurs at lower concentrations in the latter two cases. For the stability of an evaporating film the high molecular weight surfactants are most practically important. In order to obtain a more realistic description of the influence of different surfactants on the film stability we have to include in our model also the other components of the disjoining pressure (electrostatic, steric, etc.).

## ACKNOWLEDGMENTS

We are indebted to Professor I. B. Ivanov and Professor P. A. Kralchevsky for the helpful discussions. This work was supported by the “Volkswagen-Stiftung.” The authors gratefully acknowledge this support of their collaborative research.

## APPENDIX: EXACT SOLUTIONS OF THE LINEAR PROBLEMS FOR TANGENTIALLY IMMOBILE INTERFACES AND FOR SURFACTANT-FREE FILM

We outline here the exact solution of the perturbation problem given in Sec. IV.

In the particular case of tangentially immobile interface  $\mathbf{U}_f = \mathbf{0}$  and  $G_b = 1$ . Then  $a_{12} = 0$ ,  $u_h = 0$ , and  $u_s = 0$  and from Eqs. (17)–(19) the system reduces to the following first-order differential equation:

$$\frac{d \ln H_f}{d\tau} = \frac{(2\mathcal{N} + 1)(\mathcal{N} + 2H_b)}{2H_b(\mathcal{N} + H_b)^2} + \left( \frac{\mathcal{E}\mathcal{N}^2 H_b^3}{2(\mathcal{N} + H_b)^3} + \frac{\mathcal{W}}{2H_b} \right) k^2 - \frac{H_b^3}{4} (1 - \mathcal{N}) k^4,$$

for the surface shape fluctuation. After integration with respect to the dimensionless time, from 0 to a given nonper-

turbed state  $H_b(\tau)$ , using the initial condition  $H_f(0)$  for the surface shape, the general solution is readily determined to be

$$\ln\left(\frac{H_f}{H_f(0)}\right) = \left(1 + \frac{\mathcal{W}\mathcal{H}}{2\mathcal{H}+1}k^2\right)\ln\left(\frac{1}{H_b}\right) + \left(1 + \frac{3\mathcal{E}\mathcal{H}^4}{2\mathcal{H}+1}k^2\right)\ln\left(\frac{\mathcal{H}+1}{\mathcal{H}+H_b}\right) + \frac{\mathcal{W}(1-H_b)}{2\mathcal{H}+1}k^2 + \frac{\mathcal{E}\mathcal{H}^2}{2\mathcal{H}+1} \\ \times \left(\frac{1-H_b^2}{2} - 2\mathcal{H}(1-H_b) - \frac{\mathcal{H}^3(1-H_b)}{(\mathcal{H}+1)(\mathcal{H}+H_b)}\right)k^2 - \frac{1-\mathcal{S}}{2(2\mathcal{H}+1)}\left(\frac{\mathcal{H}}{4}(1-H_b^4) + \frac{1}{5}(1-H_b^5)\right)k^4.$$

In the case of surfactant-free film it follows that  $G_0=0$ ,  $G_f=0$ ,  $C_0=0$ , and  $C_f=0$ . The exact solution of the differential equation is obtained in Ref. 44, Eq. (9.6). Here we transform this expression in terms of our dimensionless parameters introduced in Sec. III. We take into account the right definition of the rescaled numbers used in Ref. 44, Eqs. (8.3b) and (9.3). The resulting expression is

$$\ln\left(\frac{H_f}{H_f(0)}\right) = \left(1 + \frac{4\mathcal{W}\mathcal{H}}{2\mathcal{H}+1}k^2\right)\ln\left(\frac{1}{H_b}\right) + \left(1 + \frac{12\mathcal{E}\mathcal{H}^4}{2\mathcal{H}+1}k^2 + \frac{4\mathcal{M}\mathcal{H}^3}{2\mathcal{H}+1}k^2\right)\ln\left(\frac{\mathcal{H}+1}{\mathcal{H}+H_b}\right) + \frac{4\mathcal{W}(1-H_b)}{2\mathcal{H}+1}k^2 \\ + \frac{4\mathcal{E}\mathcal{H}^2}{2\mathcal{H}+1}\left(\frac{1-H_b^2}{2} - 2\mathcal{H}(1-H_b) - \frac{\mathcal{H}^3(1-H_b)}{(\mathcal{H}+1)(\mathcal{H}+H_b)}\right)k^2 + \frac{4\mathcal{M}\mathcal{H}}{2\mathcal{H}+1}\left(\frac{1-H_b^2}{2} - \mathcal{H}(1-H_b)\right)k^2 \\ - \frac{2}{2\mathcal{H}+1}\left(\frac{\mathcal{H}}{4}(1-H_b^4) + \frac{1}{5}(1-H_b^5)\right)k^4.$$

It may be noted that at the rupture time  $H_f=1$  and the general solutions give one transcendental equation for the calculation of the rupture film thickness  $H_r$  as a function of the wave number  $k$ . The maximization of  $H_r$  for the full set of wave numbers  $k$  determines the critical film thickness  $H_c$  and wave number  $k_c$ .

<sup>1</sup>P. A. Kralchevsky, K. D. Danov, and I. B. Ivanov, "Thin liquid film physics," in *Foams, Theory, Measurements, and Applications*, edited by R. K. Prud'homme and S. A. Khan (Dekker, New York, 1996).

<sup>2</sup>R. R. Ramamohan and J. C. Slattery, "Effect of surface viscosity in the entrapment and displacement of residual oil," *Chem. Eng. Commun.* **26**, 241 (1984).

<sup>3</sup>J. H. Lienhard, M. Alamgir, and M. Trela, "Early response of hot water to sudden release from high pressure," *J. Heat Transfer* **100**, 473 (1978).

<sup>4</sup>T. Kashiwagi, Y. Kurosaki, and H. Shishido, "Enhancement of vapour adsorption into a solution using the Marangoni effect," *Nihon Kikai Gakkai Ronbunshu B* **51**, 1002 (1985).

<sup>5</sup>R. A. Cairncross, Ph.D. dissertation (University of Minnesota, Minnesota, 1994).

<sup>6</sup>C. S. Dunn, Ph.D. dissertation, SUNY at Buffalo, New York, 1978.

<sup>7</sup>A. Koulago, V. Shkadov, A. D. Ryck, and D. Quére, "Film entertainment by a fibre quickly drawn out of a liquid bath," *Phys. Fluids* **7**, 1221 (1995).

<sup>8</sup>S. D. Lin and H. Brenner, "Marangoni convection in a tear film," *J. Colloid Interface Sci.* **85**, 59 (1982); "Tear film rupture," *ibid.* **89**, 226 (1982).

<sup>9</sup>J. N. Israelachvili, *Intermolecular and Surface Forces* (Academic Press, London, 1985).

<sup>10</sup>Ch. Maldarelli and R. K. Jain, "The hydrodynamic stability of thin films," in *Thin Liquid Films: Fundamentals and Applications*, edited by I. B. Ivanov (Dekker, New York, 1988).

<sup>11</sup>D. Hatzivramidis, "Stability of thin evaporating/condensing films in the presence of surfactants," *Int. J. Multiphase Flow* **18**, 517 (1992).

<sup>12</sup>K. D. Danov, I. B. Ivanov, Z. Zapryanov, E. Nakache, and S. Raharimalala, "Marginal stability of emulsion thin film," in *Proceedings of the Conference of Synergetics, Order and Chaos*, edited by M. Velarde (World Scientific, Singapore, 1988).

<sup>13</sup>D. D. Joseph, *Stability of Fluid Motions*, (Springer-Verlag, New York, 1976), Vol. I.

<sup>14</sup>P. Drazin and W. Reid, *Hydrodynamic Stability* (Cambridge University Press, New York, 1981).

<sup>15</sup>A. J. Vries, "Foam stability. III. Spontaneous foam destabilization resulting from gas diffusion," *Rec. Trav. Chim. Pays-Bas.* **77**, 44 (1958).

<sup>16</sup>A. Vrij, "Possible mechanism for the spontaneous rupture of thin, free liquid films," *Discuss. Faraday Soc.* **42**, 23 (1966).

<sup>17</sup>A. Vrij and J. Overbeek, "Rupture of thin liquid films due to spontaneous fluctuations in thickness," *J. Am. Chem. Soc.* **90**, 3074 (1968).

<sup>18</sup>I. B. Ivanov, B. P. Radoev, E. D. Manev, and A. D. Scheludko, "The theory of the critical thickness of thin liquid films," *Trans. Faraday Soc.* **66**, 1262 (1970).

<sup>19</sup>D. S. Dimitrov and I. B. Ivanov, "Hydrodynamics of thin liquid films. On the rate of thinning of microscopic films with deformable interfaces," *J. Colloid Interface Sci.* **64**, 97 (1978).

<sup>20</sup>S. G. Yiantsios and B. G. Higgins, "Rupture of thin films: Nonlinear stability analysis," *J. Colloid Interface Sci.* **147**, 341 (1991).

<sup>21</sup>I. B. Ivanov, S. K. Chakarova, and B. I. Dimitrova, "Instability of emulsion liquid films induced by the transfer of acetic acid," *Colloids Surfaces* **22**, 311 (1987).

<sup>22</sup>B. I. Dimitrova, I. B. Ivanov, and E. Nakache, "Mass transport effects on the stability of emulsion films with acetic acid and acetone diffusing across the interface," *J. Dispersion Sci. Technol.* **9**, 321 (1988).

<sup>23</sup>F. J. Holly, "Wetting," in *Spreading and Adhesion*, edited by J. F. Padday (Academic Press, New York, 1978).

<sup>24</sup>J. L. Castillo and M. G. Velarde, "Marangoni convection in liquid films with a deformable open surface," *J. Colloid Interface Sci.* **108**, 264 (1985).

<sup>25</sup>R. K. Jain and E. Ruckenstein, "Stability of stagnant viscous films on a solid substrate," *J. Colloid Interface Sci.* **54**, 108 (1976).

<sup>26</sup>D. A. Edwards, H. Brenner, and D. T. Wasan, *Interfacial Transport Processes and Rheology* (Butterworth-Heinemann, Boston, 1991).

<sup>27</sup>R. J. Gumerman and G. Homsy, "Stability of uniformly driven flows with application to convection driven by surface tension," *J. Fluid Mech.* **68**, 191 (1975).

<sup>28</sup>M. B. Williams and S. H. Davis, "Nonlinear theory of film rupture," *J. Colloid Interface Sci.* **90**, 220 (1982).

<sup>29</sup>J. R. A. Pearson, "On convection cells induced by surface tension," *J. Fluid Mech.* **4**, 489 (1958).

<sup>30</sup>L. E. Scriven and C. V. Sternling, "On cellular convection driven by surface-tension gradients: Effects of mean surface tension and surface viscosity," *J. Fluid Mech.* **19**, 321 (1964).

<sup>31</sup>P. L. T. Brian, "Effect of Gibbs adsorption on Marangoni instability," *AIChe J.* **17**, 765 (1971).

<sup>32</sup>P. L. T. Brian and J. R. Ross, "The effect of Gibbs adsorption on Marangoni instability in penetration mass transfer," *AIChe J.* **18**, 582 (1972).

<sup>33</sup>C. L. McTaggart, "Convection driven by concentration- and temperature-dependent surface tension," *J. Fluid Mech.* **134**, 301 (1983).

<sup>34</sup>K. Ho and H. Chang, "On nonlinear double-diffusive Marangoni instability," *AIChe J.* **34**, 705 (1988).

<sup>35</sup>H. A. Dijkstra, "The coupling of Marangoni and capillary instabilities in

- an annular thread of liquid," J. Colloid Interface Sci. **136**, 151 (1990).
- <sup>36</sup>D. A. Goussis and R. E. Kelly, "On the thermocapillary instabilities in a liquid layer heated from below," Int. J. Heat Mass Transf. **33**, 2237 (1990).
- <sup>37</sup>D. A. Goussis and R. E. Kelly, "Surface wave and thermocapillary instabilities in a liquid film flow," J. Fluid Mech. **223**, 25 (1991).
- <sup>38</sup>C. Pérez-García and G. Carniero, "Linear stability analysis of Bénard–Marangoni convection in fluids with a deformable free surface," Phys. Fluids A **3**, 292 (1991).
- <sup>39</sup>W. Ji, H. Bjurström, and F. Setterwall, "A study of the mechanism for the effect of heat transfer additives in an adsorption system," J. Colloid Interface Sci. **160**, 127 (1993).
- <sup>40</sup>J. Berg and A. Acrivos, "The effect of surface active agents on convection cells induced by surface tension," Chem. Eng. Sci. **20**, 737 (1965).
- <sup>41</sup>H. Palmer and J. Berg, "Hydrodynamic stability of surfactant solutions heated from below," J. Fluid Mech. **51**, 385 (1972).
- <sup>42</sup>N. Imaishi, M. Hozawa, K. Fujinawa, and Y. Suzuki, "Theoretical study of interfacial turbulence in gas–liquid mass transfer, applying Brian's linear-stability analysis and using numerical analysis of unsteady Marangoni convection," Int. Chem Eng. **23**, 466 (1983).
- <sup>43</sup>S. H. Davis, "Thermocapillary instabilities," Annu. Rev. Fluid Mech. **19**, 403 (1987).
- <sup>44</sup>J. P. Burelbach, S. G. Bankoff, and S. H. Davis, "Nonlinear stability of evaporating/condensing liquid films," J. Fluid Mech. **195**, 463 (1988).
- <sup>45</sup>S. W. Joo, S. H. Davis, and S. G. Bankoff, "Long-wave instabilities of heated falling films: Two-dimensional theory of uniform layers," J. Fluid Mech. **230**, 117 (1991).
- <sup>46</sup>I. B. Ivanov and D. S. Dimitrov, "Thin film drainage," in *Thin Liquid Films: Fundamentals and Applications*, edited by I. B. Ivanov (Dekker, New York, 1988).
- <sup>47</sup>H. J. Palmer, "The hydrodynamic stability of rapidly evaporating liquids at reduced pressure," J. Fluid Mech. **75**, 487 (1976).
- <sup>48</sup>A. W. Adamson, *Physical Chemistry of Surfaces* (Wiley, New York, 1976).
- <sup>49</sup>S. S. Dukhin, G. Kretzschmar, and R. Miller, *Dynamics of Adsorption at Liquid Interfaces* (Elsevier, Amsterdam, 1995).
- <sup>50</sup>W. Ji and F. Setterwall, "On the instabilities of vertical falling liquid films in the presence of surface-active solute," J. Fluid Mech. **278**, 297 (1994).
- <sup>51</sup>R. L. Kao, D. A. Edwards, and D. T. Wasan, "Measurement of interfacial dilatational viscosity at high rates of interface expansion using the maximum bubble pressure method," J. Colloid Interface Sci. **148**, 247 (1992); "Measurement of the dynamic interfacial tension and interfacial dilatational viscosity at high rates of interfacial expansion using the maximum bubble pressure method," *ibid.* **148**, 257 (1992).